Renewable Energy, Environment, and Power Quality Journal (REE&PQJ)
ISSN:3020-531X
Volume 26, July 2026

Fast Fault Location Using Travelling-Wave Based Distance Protection

J.M. Gómez-Castillo, A. Blazquez, E. Torres, D.M. Larruskain, A. Iturregi

Department of Electrical Engineering, School of Engineering in Bilbao, University of the Basque Country EHU
Plaza Ingeniero Torres Quevedo 1, 48013 Bilbao, Spain

Abstract. Conventional protection systems rely on phasor representations that assume near-steady conditions over a power-frequency cycle, an assumption increasingly fragile under rapidly changing operating environments. These methods typically require at least one cycle to issue a trip, limiting their speed and potentially compromising system stability, particularly in networks with significant inverter-based resources and reduced inertia. Faster clearance is therefore essential to maintain secure power transfer travelling-wave techniques, which exploit the earliest high-frequency transients launched by a fault, enable sub-cycle decision-making and offer a promising foundation for fast and robust protection schemes. The paper explores the underlying principles of travelling-wave phenomena and their application to distance protection, highlighting how time-domain features can enhance speed and reliability compared with conventional phasor-based methods. Particular attention is given to high-impedance faults, assessing how the proposed ravelling-wave-based metrics can improve detection sensitivity even under severely attenuated fault currents. Finally, the proposed protection scheme is validated through a transmission system study case implemented in PSCAD, where a set of fault types and locations are examined to assess its performance, sensitivity, and robustness under diverse operating conditions.

Key words. Detection, Distance Protection, Location, Travelling-Wave, Time-Domain.

1. Introduction

Conventional protection systems are predominantly founded on the use of phasor-based representations, which involves that voltages and currents can be adequately described by their fundamental-frequency components, a linear relationship exists between them and the system remains effectively steady over the duration of a power-frequency cycle, so that phasor estimates remain valid. However, these assumptions become increasingly fragile under rapidly evolving operating conditions [1].

In conventional protection practice, phasor-based elements typically require one or one and a half fundamental cycles to issue a tripping signal following fault inception [2]. Their operating speed is constrained primarily by the interval needed to obtain enough accurate estimates of the post-fault phasors, a process that inherently limits the speed with which these elements can react.

Moreover, the timely clearance of faults is essential to preserve the dynamic security of the system; delays may compromise transient stability and, in extreme cases, precipitate widespread loss of supply. This requirement becomes even more stringent in networks with a substantial presence of inverter-based resources, where reduced inertia and limited fault-current capability diminish the system's natural resilience to disturbances. Under such conditions, even small improvements in clearing time can significantly enhance the power that the network can transfer while remaining stable, underscoring the critical value of rapid and dependable protection actions [2–3]. To address these difficulties, time-domain-based approaches have gained prominence, exploiting the very first moments of the disturbance when the signal still preserves highly informative transient features [3-5]. In this manner, dependence on detailed generator behaviour is minimised, since the action is taken before these units are able to exert a noticeable influence on the system dynamics.

Within this conceptual framework, travelling-wave protection offers a fundamentally different perspective by focusing on the earliest manifestations of a disturbance rather than on quasi-steady phasor quantities [6]. When a fault occurs, sharp voltage and current discontinuities propagate through the network at near-light velocity, carrying information largely unaffected by generator dynamics, inverter controls, or steady-state assumptions. By analysing these initial wavefronts directly in the time domain, travelling-wave schemes can reach decisions within a fraction of a cycle, avoiding the latency of forming phasor estimates and the limitations that arise under rapidly changing system conditions [7]. As modern grids become increasingly dominated by inverter-based resources and the margin for delayed fault clearance narrows, the capability of travelling-wave methods to act before the wider system responds makes them especially attractive [8]. Notable advantages include improved detection accuracy, lack of dependency on fault-current magnitude, and reliable operation even under severely limited current contribution [9]. This paper focuses particularly on high-impedance fault scenarios, where these benefits become especially relevant.

[10] presents a travelling wave-based protection algorithm validated with real case studies, but it does not analyze high-impedance faults or assess behavior at different locations or impedance conditions. [11] proposes a travelling-wave method for single phase-to-ground faults using EMTP simulations and real system parameters; however, it does not consider multi-phase scenarios combining high fault resistance with long distances, where travelling-wave signatures become harder to detect and classify. [12] presents an ultra-high-speed fault classification algorithm for double-circuit lines that uses only the first current travelling-wave group for rapid detection, classification, and phase selection with very low computational effort. The method is robust across fault impedances, though it does not perform fault location.

The paper presents a robust travelling-wave-based methodology for fast, highly sensitive, and reliable fault detection and location, integrated within a comprehensive examination of travelling-wave-based distance protection that covers both the theoretical foundations and the practical implementation of the proposed scheme. Validation is performed through a PSCAD case study involving multiple fault types and locations, enabling a detailed assessment of the method's sensitivity, selectivity, and overall dependability under diverse operating conditions.

2. Travelling-wave principles

When a transmission line is subjected to a disturbance, as shown in Fig. 1, fast electromagnetic surges propagate along the conductor, gradually losing their sharpness. They are partially reflected whenever they encounter a sudden change in electrical characteristics such as the low-impedance discontinuity created by a fault. These reflections produce voltage reversal with the corresponding current response, yielding one wave travelling away from the source and another returning towards it. Both components move at the same velocity and because this propagation speed and the attenuation are essentially frequency-independent, the travelling-wave shape is preserved and can be regarded as free from waveform distortion [6].

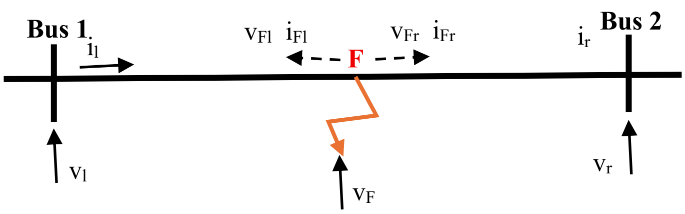

Fig. 1. Internal fault on a power line.

Equations (1) and (2) describe the voltage and current in a two-conductor, lossless transmission line, expressed in the time domain as functions of position *x* and time *t*, obtained by letting the segment length *Δx* tend to zero [2].

$$v(x,t) = F(x - ut) + f(x + ut) \quad (1)$$

$$i(x,t) = \frac{1}{Z_0}[F(x - ut) - f(x + ut)] \quad (2)$$

where:

$Z_0 = \sqrt{\frac{L}{C}}$ is the characteristic impedance of the line.

$u = \frac{1}{\sqrt{LC}}$ is the propagation velocity.

Using standard wave-separation procedures, the solution can be decomposed into a forward-propagating component, $F(x - u \cdot t)$, and a backward-propagating component, $f(x + u \cdot t)$. The forward wave is obtained by multiplying equation (1) by Z_0 and adding the result to equation (2). This component depends solely on the line's characteristic impedance Z_0 and is therefore unaffected by the termination impedance [2].

At impedance discontinuities, the behaviour of these waves is governed by the reflection and transmission coefficients, which determine the amplitude and polarity of the returning and transmitted components. In low-impedance faults, the reflection coefficient approaches –1, explaining the strong voltage reversal typically observed. Because the initial transient contains broadband, high-frequency content, its earliest arrival at each terminal carries valuable information about the fault location. The timing of this first wavefront arrival, together with its counterpart at the remote end, forms the basis of many travelling-wave-based fault-locating principles [7].

3. Travelling-wave based distance protection algorithm

The travelling-wave based distance protection proposed for this paper executes the flowchart illustrated in Fig. 2. This approach prioritizes high-speed detection by analysing the electromagnetic transients immediately following a fault.

A. Data Acquisition.

The proposed algorithm starts by measuring the instantaneous values of three-phase currents and voltages at both the local terminal (Bus 1) and the remote terminal (Bus 2).

B. Signal Processing and Filtering

The algorithm enters its most critical stage, the processing and filtering of the measurements. The primary objective of this phase is to eliminate the fundamental frequency component and isolate only the high frequency components associated with the travelling waves.

In order to decouple the phase signals and accurately analyse wave propagation, the Clarke modal transformation is first applied to separate the ground mode (0) from the aerial modes (α and β). In this regard, the α component is primarily utilized because it is inherently influenced by all three phases. Nonetheless, to ensure the algorithm is valid for all fault types, three distinct α components are calculated, each associated with a different phase (A, B and C) [12], [14].

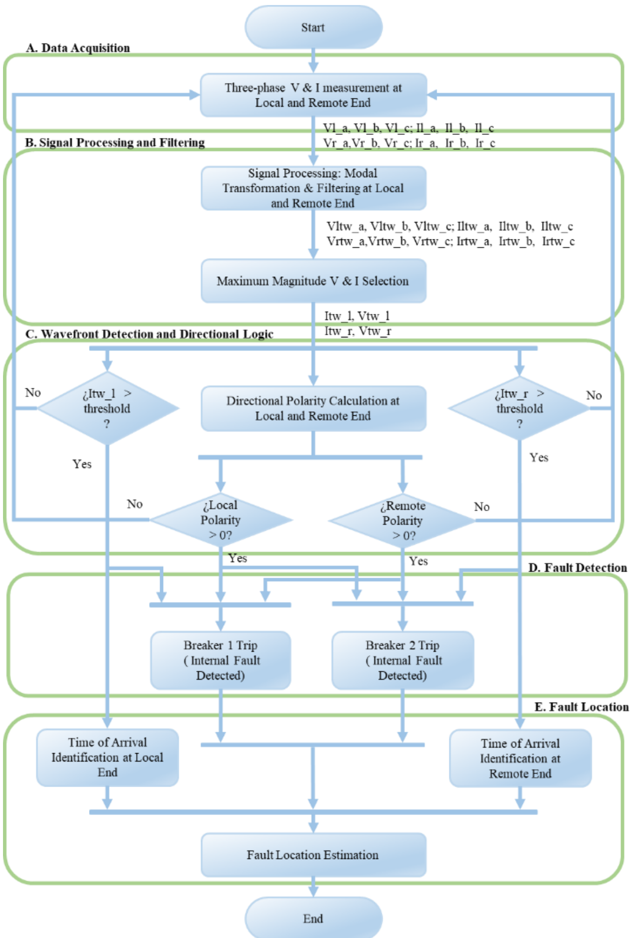

Fig. 2. Distance protection algorithm.

Subsequently, an incremental filter is applied to these three α components to extract the voltage and current travelling waves. Finally, once these travelling waves components are obtained, the algorithm selects the signal with the highest magnitude to serve as the final voltage or current representation, V_{tw} and I_{tw}, obtained after the comprehensive processing, filtering and selection performed at both terminals [14].

C. Wavefront Detection and Directional Logic

Once the processed and filtering signals are obtained, the algorithm simultaneously executes the detection of the initial wavefront and calculation of the directional polarity through a series of analytical comparison.

On the one hand, to detect the first travelling wave, the magnitude of the signal is compared against a predefined threshold. In the event that the signal exceeds this value, it is validated as the first travelling wave detection. Otherwise, the condition is not met, the algorithm resets to the initial three phase measurement stage.

On the other hand, the directional function logic (TW32) is implemented by calculating the torque at each terminal. Specifically, this value is integrated over a few microseconds, as represented by (4) [7].

$$Torque\ integrated = -\int_0^{\Delta t} I_{tw} \times V_{tw} \qquad (4)$$

Consequently, if the integral of the torque is positive, the fault is identified as forward (internal), and the protective element is authorized to act. Conversely, a negative integral indicates a reverse fault (external), causing the algorithm to return to the acquisition signals stage. This ensures high selectivity, allowing the protection to operate only for faults located within the protected line segment [7].

D. Fault Detection

In this context, once the required tripping conditions are satisfied, the algorithm coordinates the operation of circuit breakers CB 1 and CB 2, at both ends of the line. For a trip command to be issued, four specific criteria, based on the processed current travelling waves, must be met:

1. Detection of the first current wavefront at the local bus.
2. Detection of the first current wavefront at the remote bus.
3. Local Polarity must be positive
4. Remote Polarity must be positive

By fulfilling these requirements, the system ensures that the fault has occurred strictly within the protected line.

E. Fault Location

Finally, if CB 1 and CB 2 have been tripped, the algorithm proceeds to estimate the fault distance from the local terminal (Bus 1). To achieve this, the system first identifies the precise arrival timestamps (t_l and t_r) of the first wavefront at each end of the line. Subsequently, the location is calculated using the following double-ended expression:

$$Distance = \frac{1}{2} \times (LL + u \times (t_l - t_r)) \qquad (5)$$

Where:
LL is the total length of the protected transmission line, u is the propagation velocity of the travelling wave, and t_l and t_r are the arrival times of the first wavefront at the local and remote terminals respectively.

4. Study case

To evaluate the effectiveness and robustness of the proposed travelling wave based distance protection, a series of simulations are conducted using PSCAD/EMTDC environment. This section first describes the electrical grid model used for the validation. Subsequently, a detail analysis of a specific phase-to-phase fault is presented to illustrate the algorithm's internal operation, followed by an extensive performance assessment covering different fault locations and selectivity scenarios to demonstrate the method's reliability under diverse operating conditions.

A. Grid Model Description

To validate the protection distance algorithm, a two terminal transmission system is implemented in the PSCAD/EMTDC environment, as illustrated in Fig 4. The 230 kV, 60 Hz model incorporates two three-phase AC sources, a 100 km transmission line, between Bus 1 and

Bus 2, with 20 km line segments at both ends, enabling the evaluation of protection selectivity against both internal and external faults via the controlled operation of circuit breakers B1 and B2.

Furthermore, power flow is established by a 20 degrees phase shift between the remote source (B) and the local source (A), with each source characterized by a short circuit power of $S_{cc} = 1000\,\text{MVA}$. In this context, the model integrates a fault generation logic capable of simulating various scenarios. Finally, instantaneous voltage and current measurements are captured at both ends of Line1 to test the performance of the proposed protection algorithm.

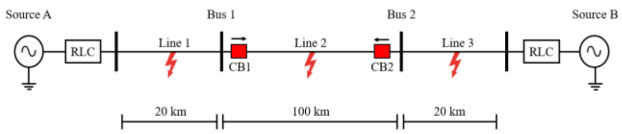

Fig. 3. Base model for distance protection algorithm validation.

B. B-C Fault Case Study

To demonstrate the effectiveness of the proposed methodology, a specific case study is analysed in detail. Given that the operational sequence remains consistent across all simulated scenarios, a phase-to-phase (B-C) fault is selected as a representative example. This fault is characterized by zero fault resistance and is located at a distance of 60 km from the local terminal (Bus 1). Furthermore, to evaluate the dynamic response, fault inception is 0.2 s with a total duration of 0.08 seconds.

Once the three-phase signals are captured, the algorithm applies the Clarke transformation and filtering. As a result, the fundamental frequency component is effectively eliminated, allowing the high frequency transients associated with the travelling waves to be isolated. As shown in Fig 4, the processed voltage and current signals at both, local and remote terminals, exhibit clear incremental spikes at the fault inception. In this regard, these increments represent the travelling wave, providing the essential data for the subsequent detection and directional logic.

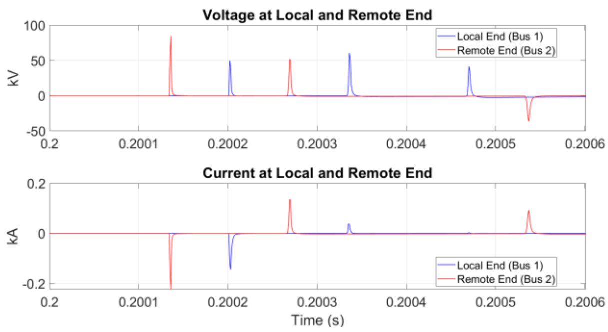

Fig. 4. Processed and filtered V & I at local terminal.

Regarding the detection stage, the algorithm monitors the magnitude of the isolated waves. In this case study, the wavefronts of voltage and current signals at both terminals exceed the predefined threshold of 0.003 kA and kV. Consequently, the first arrival of the travelling wave is successfully identified.

Simultaneously, the directional logic is evaluated by integrating the product of the travelling wave voltage and current. At the local terminal (Bus1), the initial voltage wavefront is positive, while the current wavefront is negative. Although their product is negative, the negative sign included in torque integrated expression, as defined in (4), results a positive polarity (Fig 5). Similarly, at the remote terminal, the voltage is positive and the current is negative, therefore, the calculation also yields a positive polarity (Fig 5). By achieving a consistent positive result at both ends, the disturbance is confirmed as an internal fault.

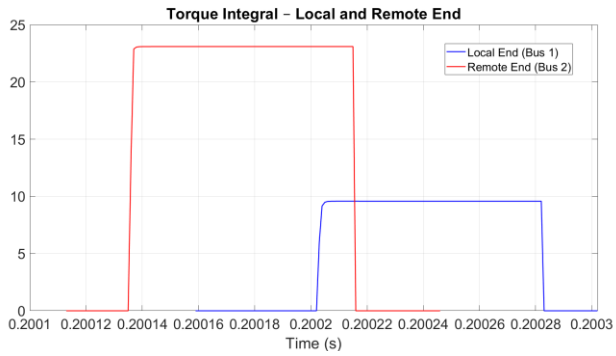

Fig. 5. Polarity detection via torque integral at local and remote end.

Once the wavefronts are detected and the internal nature of the fault is confirmed, the trip command is issued. As observed in the results, both CB 1 and CB 2 operate simultaneously.

It is important to highlight that the first wavefront reaches the local terminal 0.203 ms and the remote terminal 0.136 ms after fault inception. Due to the requirement that all four conditions (detection and polarity at both ends) must be strictly satisfied before acting, the circuit breakers trip with a slight delay of 0.204 ms after fault inception at 0.2 s, Fig 6. This latency reflects the time required for the travelling waves to reach the protections and for the communication based directional logic to validate the internal fault.

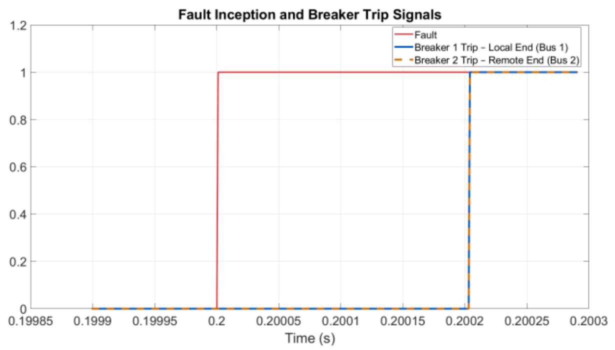

Fig. 6. CB trip signals vs fault inception.

Finally, after the circuit breakers have been tripped, the fault location is estimated using the recorded arrival timestamp. By utilizing t_l=200.203 and t_r=200.136 ms (Fig 7) within the double ended expression (5), the fault is located at 60.040274 km from the local terminal (Bus 1) (Fig 8).

Comparing this result to the actual fault distance of 60 km, the algorithm achieves a remarkably high precision, with an absolute error of 40.27 m, which corresponds to a relative error of only 0.067 %. Thus, these findings demonstrate the robustness of the travelling wave approach for fast and accurate fault location in transmission lines.

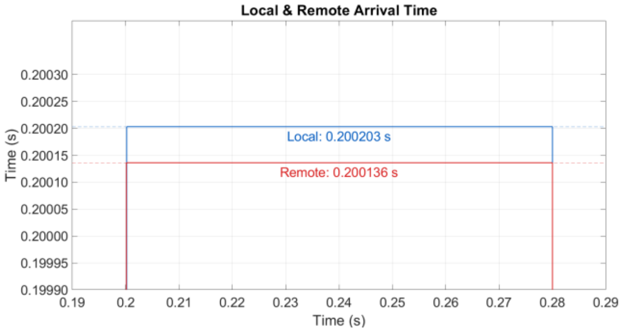

Fig. 7. Local and remote arrival time.

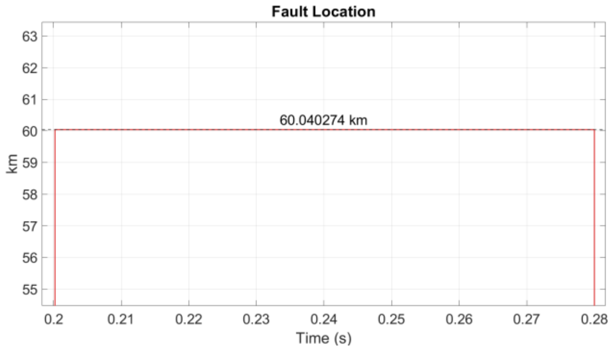

Fig. 8. Estimated distance.

C. *Sensitivity and Selectivity Analysis*

To validate the proposed protection and location strategy, several fault scenarios are simulated by varying the fault type, location, and fault resistance, within the protected line. The results, summarized in Table 1, demonstrate the algorithm's high reliability in both fault detection and distance estimation.

Table 1. Fault detection and location results under various conditions.

		FAULT LOCATION					FAULT DETECTION
FAULT TYPE	FAULT RESISTENCE (Ω)	REAL LOCATION (km)	ESTIMATED DISTANCE (km)	FAULT LOCATION ERROR (%)	LOCAL ARRIVAL TIME t_l (ms)	REMOTE ARRIVAL TIME t_r (ms)	TRIPPING TIME (ms)
A-G	0	10	9,99	0,112	200,036	200,303	0,304
		60	60,04	0,067	200,203	200,136	0,204
	50	10	9,99	0,112	200,036	200,303	0,304
		60	60,04	0,067	200,203	200,136	0,204
	500	10	9,84	1,611	200,036	200,304	0,305
		60	60,04	0,067	200,203	200,136	0,204
B-C	0	10	9,99	0,112	200,036	200,303	0,304
		60	60,04	0,067	200,203	200,136	0,204
	50	10	9,99	0,112	200,036	200,303	0,304
		60	60,04	0,067	200,203	200,136	0,204
	500	10	9,99	0,112	200,036	200,303	0,304
		60	60,04	0,067	200,203	200,136	0,204
A-B-C	0	10	9,99	0,112	200,036	200,303	0,304
		60	60,04	0,067	200,203	200,136	0,204
	50	10	9,99	0,112	200,036	200,303	0,304
		60	60,04	0,067	200,203	200,136	0,204
	500	10	9,99	0,112	200,036	200,303	0,304
		60	60,04	0,067	200,203	200,136	0,204

Regarding fault location, it can be observed that the relative error remains very low across all scenarios, ranging from values below 0,12 % in most conditions to a single higher deviation to 1.61 % for the 500 Ω and 10 km fault case, which is still remarkably accurate considering the high-impedance nature of the fault. Notably, when maintaining a fixed fault location (measured from the local end as shown in the 'Real Location' column), the arrival times of the first wavefront at both terminals (t_l and t_r) remain practically constant, regardless of the fault type or the resistance value.

Regarding fault detection, the data shows that the algorithm successfully identifies all internal events. In terms of detection speed, the results highlight the ultra-high-speed nature of the proposed protection scheme. For a fault located at 60 km from the local bus, the trip command is issued just 0.204 ms after the fault inception. In contrast, for a fault closer to the local terminal (at 10 km), the tripping time is 0.304 or 0.305 ms. The influence of the fault impedance on the results is minimal.

Furthermore, the algorithm's ability to discriminate between internal and external faults is tested to ensured selectivity. According to Table 2, the scheme demonstrates 100 % reliability. Specifically, for faults located in adjacent lines (Line 1 and Line 3), the directional logic detects a negative polarity at one of the terminals, thereby inhibiting the trip command. Conversely, for all internal events, the consistent positive polarity at both ends ensures a secure ultra-high-speed operation, with an average tripping time of 0.204 ms.

Table II. Selectivity analysis for internal and external faults.

INTERNAL/EXTERNAL SELECTION					
FAULT TYPE	EXT. FAULT LINE 1	INT. FAULT LINE 2	EXT. FAULT LINE 3	TRIP CB 1	TRIP CB 2
A-G	YES	NO	NO	NO	NO
B-C	NO	YES	NO	YES	YES
A-B-C	NO	NO	YES	NO	NO

D. *Comparison with differential protection*

In this section, the proposed algorithm is compared with the differential protection principle, as it constitutes the benchmark scheme for transmission line protection in terms of reliability and selectivity [15].

Both travelling-wave-based protection schemes with communication and differential protection rely on information from both ends of the transmission line, requiring communication channels to ensure coordinated operation. In both approaches, the protection decision is based on a comparison of electrical quantities at both ends, enabling inherent selectivity between internal and external faults. Furthermore, both methods benefit from synchronized measurements to enhance accuracy and reliability and aim to provide high-speed fault detection while maintaining dependability under varying system operating conditions.

Table III compares both approaches in a general manner across key aspects. Differential protection is based on fundamental-frequency quantities and provides fast and robust fault detection, whereas travelling-wave methods rely on high-frequency transients, enabling faster operation and additional capabilities such as fault location, with stricter measurement requirements. Unlike travelling-wave-based methods, differential protection is not inherently designed for fault location, as its primary function is the discrimination between internal and external faults rather than the estimation of fault position,

Table III. Comparison between travelling-wave-based protection and differential protection.

	Travelling Wave (with communication)	Differential Protection
Signals	Transient components (kHz–MHz)	Fundamental frequency (50/60 Hz)
Sample frequency	1 MHz	1.2 – 10 kHz
Operating Speed	Very high (µs–sub-ms)	High (ms)
Fault Location	Precise fault location	Not inherent
Model Dependence	Low	Moderate
CT Saturation	Low sensitivity	High sensitivity
Typical Application	HVDC, long lines, IBR-based systems	Conventional AC networks

This comparison is illustrated through a single-phase fault case study, as this is the most common fault in power systems. A single-phase-to-ground (AG) fault is simulated at 60 km from the local terminal. A differential protection scheme which monitors currents at both ends calculates their difference has been implemented on the simulation model described in Fig 3, retaining the same system parameters and operating conditions used throughout this study. When the differential current exceeds a predefined threshold, the fault is classified as internal, and a trip signal is issued.

Table IV. Comparison for AG fault at 60 km.

Protection Principle	Fault Resistance (Ω)	Detection time (ms)
Differential	0	3.62
	50	4.16
	500	5.7
Travelling wave [Proposed method]	0	0.204
	50	0.204
	500	0.204

The detection times obtained for both protection schemes are summarized in Table IV for three fault resistance values: 0 Ω, 50 Ω, and 500 Ω. The results reveal two notable differences between the approaches. Firstly, the proposed travelling-wave-based method achieves significantly faster fault detection across all fault resistance values. Secondly, while the proposed method maintains consistent performance regardless of fault resistance, the detection time of the differential protection scheme increases with fault resistance. This degradation is attributed to the attenuation of the differential current signal as fault resistance increases, which delays threshold crossing. In contrast, the travelling-wave-based method relies on high-frequency transients generated at the instant of fault inception, whose propagation characteristics are largely independent of fault resistance, thus ensuring robust and consistent detection performance.

5. Conclusion

This paper has presented a travelling-wave based distance protection methodology characterized by its high speed and precision. Based on the obtained results, it is concluded that the algorithm is remarkably robust, successfully identifying internal faults in a time range between 0.204 and 0.305 ms after fault inception. Notably, the system's performance under high-impedance fault conditions of up to 500 Ω is outstanding. In these scenarios, the proposed filtering strategy and the torque integral based directional logic have demonstrated superior robustness and stability, maintaining fault location errors below 1.61% even under this critical circumstance. Furthermore, the selectivity analysis confirms that the implemented logic effectively discriminates between internal and external events with 100% reliability.

Finally, regarding future work, it is proposed to extend this study to the analysis of power systems with a high penetration of power electronic converters. In this regard, further research will evaluate how inverter control strategies affect fault detection capabilities and location accuracy. The ultimate goal is to ensure protection resilience in future low-inertia grids

Acknowledgement

This work has been funded by the Basque Government via RESINET+ project grant (KK-2025-00100) and GISEL Research Group grant (IT1799-26).

References

[1] T. Russell, P. Bhattarai, M. Cox, M. Quinteros, and T. Field, “Implementation and analysis of a digital model of the incremental-quantity distance element using EMTP” in 2023 76th Annual Conference for Protective Relay Engineers.

[2] E. O. Schweitzer, B. Kasztenny, A. Guzmán, V. Skendzic, and M. V. Mynam, “Speed of line protection-can we break free of phasor limitations?” SEL, Atlanta, Georgia, Tech. Rep., Aug. 2015.

[3] B. Kasztenny, “Improving Line Crew Dispatch Accuracy When Using Traveling-Wave Fault Locators”, 46th Annual Western Protective Relay Conference, Spokane, Washington, October 22–24, 2019.

[4] H. Kong, W. Cong, H. Zhang, M. Chen and Z. Wei, "Traveling Wave Protection of High-Voltage Transmission Line based on Waveform Similarity," 2020 IEEE/IAS Industrial and Commercial Power System Asia (I&CPS Asia), Weihai, China, 2020, pp. 1000-1005, doi: 10.1109/ICPSAsia48933.2020.9208419.

[5] E.O. Schweitzer, B. Kasztenny, Ma.V. Mynam, N. Fischer, A. Guzman "Solving Line Protection Challenges with Transient-based Relays", PACWorld. Available: https://www.pacw.org/solving-line-protection-challenges-with-transient-based-relays, accessed on 4 February 2026.

[6] P. A. Crossley and P. G. McLaren, "Distance Protection Based on Travelling Waves," in IEEE Transactions on Power Apparatus and Systems, vol. PAS-102, no. 9, pp. 2971-2983, Sept. 1983, doi: 10.1109/TPAS.1983.318102.

[7] ENTSO-E, “Use of Travelling Waves Principle in Protection Systems and Related Automations”, 2021. Available: https://eepublicdownloads.entsoe.eu/clean-documents/SOC%20documents/USE_OF_TRAVELLING_WAVES_PRINCIPLE_IN_PROTECTION_SYSTEMS_AND_RELATED_AUTOMATIONS.pdf, accesed on 4 February 2026.

[8] E. O. Schweitzer, B. Kasztenny and M. V. Mynam, "Performance of time-domain line protection elements on real-world faults," 2016 69th Annual Conference for Protective Relay Engineers (CPRE), College Station, TX, USA, 2016, pp. 1-17, doi: 10.1109/CPRE.2016.7914904.

[9] F. Wilches-Bernal *et al.*, "A Survey of Traveling Wave Protection Schemes in Electric Power Systems," in *IEEE Access*, vol. 9, pp. 72949-72969, 2021, doi: 10.1109/ACCESS.2021.3080234.

[10] A. Di Tomasso, G. Invernizzi, and G. Vielmini, ‘‘Accurate single-end and double-end fault location by traveling waves: A review with some real applications,’’ AEIT Int. Annu. Conf. (AEIT), Sep. 2019, pp. 1–6.

[11] X. Dong, J. Wang, S. Shi, B. Wang, B. Dominik, and M. Redefern, ‘‘Traveling wave based single-phase-to-ground protection method for power distribution system,’’ CSEE J. Power Energy Syst., vol. 1, no. 2, pp. 75–82, Jun. 2015

[12] I. Mousaviyan, S. Ghodratollah Seifossadat, M. Saniei, “An Ultra-High-Speed Algorithm for Fault Classification in Double Circuit Transmission Lines Using Only the First Group of Received Current Traveling Waves” Electric Power Systems Research, Vol. 206, 2022, 107841, doi.org/10.1016/j.epsr.2022.107841.

[13] B. Kasztenny, A. Guzman, N. Fischer, M. Mynam, D. Taylor, Douglas “Practical Setting Considerations for Protective Relays That Use Incremental Quantities and Traveling Waves” 2016. Available: https://selinc.com/api/download/117051, accessed on 30 March 2026.

[14] E. O. Schweitzer, A. Guzmán, M.V. Mynam, V. Skendzic, B. Kasztenny “Locating Faults by the Traveling Waves They Launch” 67th Annual Conference for Protective Relay Engineers, March 2014.

[15] R. Cimadevilla, J. García-Villalobos, “Improvements in Line Differential Relays”, PAC World, nº 51, pp. 54-59**,** March 2020.